Current Research in Biotechnology 7 (2024) 100174

Contents lists available at ScienceDirect

Current Research in Biotechnology

journal homepage: www.elsevier.com/locate/crbiot

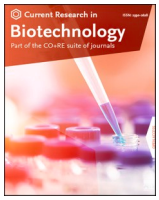

Effect of inhibiting PDHα1 gene expression on the metabolism of fatty liver cells

Xiaoguang Chen *, Qiongxia Lv, Haonan Li, Zhe Wang, Yuxin Chang

Animal Science and Technology School, Henan University of Science and Technology, 263# Kaiyuan Avenue, Luoyang 471023, China

ARTICLE INFO

Keywords:
Pyruvate dehydrogenase
Fatty liver cells
RNA interference
Glucose metabolism
Lipid metabolism

ABSTRACT

PDHα1 gene encodes catalytic subunit PDHE1α of pyruvate dehydrogenase (PDH) complex. Based on previous studies, it is hypothesized that inhibition of PDH activity prevents the entry of glycolytic pyruvate into TCA cycle, while promotes fatty acid oxidation and reduces liver triglyceride (TG) level, thereby alleviating nonalcoholic fatty liver disease (NAFLD). In this study, an in vitro model for NAFLD was established with medical fat emulsion; the most effective siRNA for PDHα1 gene was screened out by qPCR technology; the alterations in metabolism of glucose and lipid, and structure & function of mitochondria in the NAFLD cells were primarily evaluated after transfecting PDHα1 siRNA. As the results showed, after inhibiting the expression of PDHα1 gene, glucose level in culture medium was time-dependently increased, and LDH activity in the cells was moderately elevated after 24 h of transfection and then returned to the normal level after 48 h; intracellular TG level was decreased while LPS activity was increased in a time-dependent manner; no significant change in mitochondrial structure was observed with or without siRNA transfection, and ATP content was obviously reduced after 24 h of transfection, followed by restoration after 48 h. It can be concluded that inhibiting PDHα1 gene in fatty liver cells enhances lipid degradation, and represses the utilization of glucose to an extent, thus reducing TG level without impacting energy generation required for cell survival.

Introduction

Nonalcoholic fatty liver disease (NAFLD) is a continuous spectrum of diseases characterized by excessive deposition of fat in the liver accompanied with diffuse hepatic cell bullous steatosis caused by the factors other than alcohol and other known liver injury-related factors (Farrell et al., 2007; Targher and Byrne, 2017). In turn, hepatic steatosis further aggravates liver metabolic disorders, or even develops into liver fibrosis and cirrhosis, exacerbating liver damage if not given proper treatment (Monteillet et al., 2018).

Nowadays, it has been widely accepted that intrahepatic lipid accumulation caused by various factors (excessive liver fat synthesis, insulin resistance, inflammation, mitochondrial dysfunction, gut microbiota and adipokines), together with the increased de novo fatty acid synthesis, the reduced fatty acid oxidation (FAO) and the blocked liver lipid efflux ultimately cause the occurrence of fatty liver disease (Ratziu et al., 2016; Matsumoto et al., 2018). Obviously, the formation of fatty liver is closely related with the abnormality of lipid metabolism. Accordingly, how to improve the degradation and transportation of intrahepatic lipid is of great significance in preventing the occurrence of fatty liver. It is noteworthy that mitochondria, also called powerhouses of the cells, play an important role in the regulation of fat metabolism and inflammatory response (Ni et al., 2015). As an example, it has been found that adding MitoQ, one mitochondrial-targeted antioxidant, could strongly rescue mitochondrial function and attenuate the development of fatty liver disease by decreasing pathogenic alterations of cardiolipin content, an unique mitochondrial phospholipid playing a key role in mitochondrial bioenergetics (Fouret et al., 2015).

Eukaryotic cell metabolism is an exquisite combination of energy-yielding process (i.e., glycolysis and oxidative phosphorylation) and energy-consumption process (macromolecule synthesis, ion gradient maintenance) (Buttgereit and Brand, 1995; Lane and Fan, 2015; Pelletier et al., 2018). Normally, cellular ATP is yielded mainly through mitochondrial tricarboxylic acid (TCA) cycle, and oxidative phosphorylation coupled to electron transfer. During this process, acetyl CoA (AcCoA), the primary substrate for TCA cycle, is converted from glucose-derived pyruvate by the catalysis of pyruvate dehydrogenase complex (PDHC) in mitochondria (Patel et al., 2012; Stacpoole, 2017). The core

* Corresponding author.
E-mail address: chenxg8006@haust.edu.cn (X. Chen).

https://doi.org/10.1016/j.crbiot.2023.100174
Received 4 September 2023; Received in revised form 16 December 2023; Accepted 26 December 2023
Available online 27 December 2023

components of PDHC consist of multiple copies of three enzymes including enzyme E1 (TPP-dependent pyruvate dehydrogenase, PDH), E2 (dihydrolipoamide acetyltransferase) and E3 (NAD-dependent dihydrolipoamide dehydrogenase). And enzyme E1 (that's PDH) is a heterodimers composed of two PDHA1-encoding α subunits and two PDHB-encoding β subunits, and binds thiamine pyrophosphate (TPP) (Ciszak et al., 2001). PDH does not occur alone in mitochondria, but functions in the form of PDHC. As the rate-limiting enzyme, PDH complex catalyzes the irreversible oxidative decarboxylation of pyruvate to AcCoA and reduces NAD^+ into NADH, which thus links glycolytic activity with tricarboxylic acid cycle, playing an important role in energy metabolism of mitochondrial respiratory chain (Butterworth, 1989; Cooney et al.,1990; Wang et al., 2019).

Studies have confirmed that PDH deficiency causes a series of pathological changes, including mitochondrial energy metabolism disorder. For instance, PDH deficiency in infancy led to the conversion of pyruvate to lactate, subsequently inducing different degrees of metabolic acidosis (Patel et al., 2012). The fact that ketogenic diet has been proposed as an well-established therapeutic treatment for PDH-deficient patients is because this therapy not only provides fatty acid oxidation (FAO)-derived AcCoA, but reduces the adverse effects of lactic acidosis through weakening the glycolytic process, and minimizing the level of pyruvate and lactate (Sofou et al., 2017). However, further research showed that hepatic specific *pdha1*-KO hepatoblastoma (HB) presented severe lactic acidosis without impacting the proliferative capacity of hepatocytes and only modestly impairing their growth, which demonstrates that, even under the most demanding circumstances, normal or neoplastic proliferation is hardly affected despite completely severing the link between glycolysis and TCA cycle (Jackson et al., 2017).

After cutting off the link between glycolysis and the TCA cycle through inactivating PDH, how does the cell make acetyl-CoA for supporting the TCA cycle and generating ATP? Based on the above researches, we raise a proposal that specifically inhibiting hepatic PHDα1 gene expression in fatty liver cells would block the entry of glycolytic pyruvate into the TCA cycle, promote fatty acid oxidation and reduce liver triglyceride level, thereby alleviating fatty liver disease. Accordingly, this study firstly established an in vitro cell model of NAFLD, then inhibited the expression of PDHα1 gene in the cells with the efficient siRNA fragment, exploring the effect of interfering PDHα1 gene on cellular metabolism, and mitochondrial structure and function in fatty acid cells, thus laying down a theoretical foundation for further research on metabolic mechanism of fatty liver development and the potential therapeutic target for NAFLD.

Materials and methods

Materials

Rat liver cell line BRL-3A used in this experiment was donated by Henan Normal University Henan Key Laboratory of Biotechnology; 20 % medical fat emulsion (MFE) was purchased from Fubicheng Pharmaceutical Technology Co., Ltd; MTT kit was from Shanghai Shenggong Biotechnology Co., Ltd; Triglyceride (TG) kit and lipase (LPS) detection kit were from Nanjing Jiancheng Bioengineering Institute; Oil red O (ORO) staining kit, LDH detection kit, and glucose detection kit were all from Shanghai Beyotime Biotechnology Co., Ltd; ATP detection kit, Rabbit anti-rat PDHα1 antibody and Cy3-labeled goat anti-rabbit IgG were respectively from Boxbio company, Abclonal and Servicebio.

Preparation of MFE working solution

20 % MFE stock solution was diluted separately into 4 %, 2 %, 1 % and 0.5 % using DMEM complete culture containing 10 % FBS, and stored at 4℃for use.

Selection of optimal concentration of MFE agent

BRL-3A cells at logarithmic growth phase were seeded in a 96-well plate in 1×10^4 cells per well. The cells were assigned into five groups: control group, 0.5 %, 1 %, 2 % and 4 % MFE-treated groups. The cells in control group were cultured by replacing MFE with an equal volume of culture medium. After 24 h of incubation, cell viability was detected for determining the optimal concentration of MFE by using MTT method.

Establishment of an in vitro model for NAFLD

The cells in logarithmic phase were harvested from plates and collected, and then prepared as a cell suspension of 5×10^5 cells/mL, and a total of 2 mL suspension was inoculated into each well of a 6-well culture plate and cultured at 37℃ in a humidified incubator with 5 % CO_2. After cells adhered to the wall, the medium was changed to one containing the optimal concentration of MFE. After 24 h and 48 h of incubation, oil red O (ORO) staining was performed to observe lipid droplet in the cells.

Screening of efficient rat PDHα1 gene siRNA fragment

According to rat PDHα1 gene sequence provided by the GenBank database (NM_001004072.2), a total of three PDHα1 siRNA fragments were designed by Oligonucleotide RNAi Designer software, and synthesized by Shanghai Sangon Biotech Co., Ltd. (Table 1). Three siRNA candidates were transfected into in vitro fatty liver cells using Lipo8000 transfection reagent. GFP expression was observed under fluorescence microscope after 8 h of transfection. After 24 h, qRT-PCR was carried out for evaluating interference efficiency of three siRNA fragments based on the relative level of PDHα1 mRNA. Primer sequences of PDHα1 and GAPDH genes were designed and synthesized by Shanghai GeneCore BioTechnologies Co., Ltd (Table 2).

siRNA transfection

The logarithmic growth phase cells were seeded in a 6-well plate at 5×10^5 cells/well and cultured until reaching 70–80 % confluence, then developed into fatty liver cells according to above protocol. The efficient siRNA was transfected into fatty liver cells as follows: for each well in a 6-well plate, 100 pmol siRNA was gently mixed with 125 μl of antibiotic- and serum-free DMEM medium, and incubated for 20 min at room temperature, followed by adding 4 μl of Lipo8000. After mixing thoroughly, siRNA-Lipo mixture was placed in room temperature for at least 6 h. 125 μl siRNA-Lipo mixture was uniformly added into each well containing cells and medium. And the cells were cultured and collected after 24 and 48 h of culture, respectively.

Immunofluorescent staining observation

Immunofluorescence staining was employed to examine the expression of PDHα1 gene. To specific, after siRNA transfection for 24 h and 48 h, cell climbing films in a 12-well plate were fixed for 15 min with 4 % paraformaldehyde and permeated with 0.3 % Triton X-100. Then, 10 %

Table 1
The designed siRNA sequence targeting rat PDHα1 gene.

	Sequence (5′-3′)
PDHα1 siRNA1	F: GCGGAUCAAUGCACAUGUAdTdT
	R: UACAUGUGCAUUGAUCCGCdTdT
PDHα1 siRNA2	F: GCAAGUGUUGAAGAAUUAAdTdT
	R: UUAAUUCUUCAACACUUGCdTdT
PDHα1 siRNA3	F: GGUACUUCAGUCACUUCAAdTdT
	R: UUGAAGUGACUGAAGUACCdTdT

Note: F: forward; R: reverse.

Table 2
The qRT-PCR primers used in this work.

Gene	Primer sequence (5′→3′)
GAPDH	FP: ACAGCAACAGGGTGGTGGAC RP: TTTGAGGGTGCAGCGAACTT
PDHα1	FP: TCCATGAGGAAGATGCTTGCCG RP: ACACAAGTGACAGAAACCACGA

normal goat serum was incubated to block non-specific binding sites for 30 min at room temperature. The cells were incubated with rabbit anti-rat primary antibody PDHα1 (1:100) overnight at 4℃, then with Cy3-labeled goat anti-rabbit IgG (1:300) for 1 h at room temperature. DAPI was added for nuclei staining for 10 min at room temperature. Finally, the sections were sealed with anti-fluorescence quenching sealing solution and observed under a fluorescence microscope.

Detection of lactate dehydrogenase (LDH) activity

The cells in logarithmic growth phase were seeded in 96-well plates at a density of 1×10^4 cells/well. After adhered to the plate walls, an in-vitro NAFLD model was established as described above. After siRNA transfection, cell culture supernatant was removed as much as possible. After adding the 150 μl 1 × diluted LDH release reagent, mix by gently shaking the plate for several times, and then continue incubation for 1 h. Cell culture plate was centrifuged, and 120 μl supernatant from each well was taken and transferred to a new 96-well plate, followed by adding 60 μl LDH working solution. Mix well and incubate at 25℃ in the dark for 30 min. Absorbance of all samples (OD value) was measured at 490 nm according to instructions provided with LDH assay kit. LDH activity (mU) was calculated according to the standard curve equation established as follows: $y = 0.0005x + 0.08$ ($R^2 = 0.9856$), in which x and y stand for LDH activity (mU) and OD value, respectively.

Detection of glucose content

The cell culture supernatants in each group were collected for measuring the amount of glucose by O-toluidine method according to glucose assay kit instructions. The absorbance value of supernatants from different groups was detected at 630 nm, and glucose content was calculated according to the standard curve equation built using the standard sample provided by the manufacturer. The equation is as follows: $y = 0.0021x + 0.2544$ ($R^2 = 0.9982$), in which x represents glucose content (mg/dl), y represents OD value.

Quantification of triglyceride (TG) content and lipase (LPS) activity

The cells in each group were harvested from plates and collected, and then prepared into cell suspension, followed by centrifuged at 1000g for 10 min for discarding the supernatant. The centrifuged cell sediment was washed twice in PBS and lysed by adding 1 % Trixton X-100. According to the instructions of the TG assay kit based on GPO-PAP enzyme method and the LPS assay kit based on methyl halide substrate method, the absorbance values were detected at 510 nm and at 580 nm using a microplate reader, respectively. Finally, triglyceride content (mmol/L) and LPS activity (U/L) were evaluated according to the formula provided by the corresponding instructions.

Observation of mitochondrial ultrastructure

After transfection of 24 h and 48 h, the culture medium was removed, and electron microscope fixative was added for fixing at 4℃. After 4 h, the fixed cells were centrifuged, followed by the removal of the supernatant. The precipitation was re-suspended and washed in PBS buffer. The cells were fixed with 1 % osmic acid and then rinsed in PBS, followed by gradient dehydration at room temperature. Different ratio of embedding agents were prepared for resin penetration and embedding, oven at 37℃ overnight. The embedding model with samples were moved into 60℃ oven to polymerize for 48 h. The resin blocks were sliced to 60 nm thin, followed by uranium-lead double staining. After dried at room temperature, the samples were observed under a transmission electron microscope (TEM).

ATP level detection

The established in vitro NAFLD cells were treated with the transfection mixture containing the effective siRNA fragment. After transfection of 24 h and 48 h, the cells were harvested from plates and collected, then lysed by ultrasonic disruption. After centrifuged for 3 min at 10000 × g, the supernatant was collected for ATP level measurement using ATP content assay kit according to the manufacturer's instructions. Noting: the absorbance of NADPH at 340 nm is proportional to intracellular ATP content. All experiments were performed three times and total ATP levels were expressed as μmol/10^6 cells.

Statistical analysis

All the data were expressed as mean ± SD and all experiments were independently repeated three times. The data analysis was performed using SPSS19.0 Software. Differences among experimental groups were analyzed by One-way ANOVA followed by the Dunnett's multiple comparison tests. A cutoff P value of < 0.05 was considered as statistically significant difference.

Results

Screening of optimal MFE concentration for inducing cell steatosis

To select one optimum inducing concentration, this study detected the effect of different concentrations of MFE on the viability of BRL-3A cells by using MTT assay. As a result, compared with the control group, cell viability was significantly reduced after 24 h of treatment with different dosages of MFE (except 0.5 %, $P < 0.05$); after exposure of 48 h, number of living cells was further decreased, and cell viability was much lower than that of 24 h. According to the data, cell viability in both 1 % MFE group for 24 h and 0.5 % MFE group for 48 h were above 75 % which can provide enough cell number for subsequent experiments (Fig. 1).

Furthermore, lipid droplets in the cells exposed to 0.5 % and 1 % MFE were detected by ORO staining. As shown in Fig. 2, only a small amount of lipid droplets were observed in the normal cells (Fig. 2A).

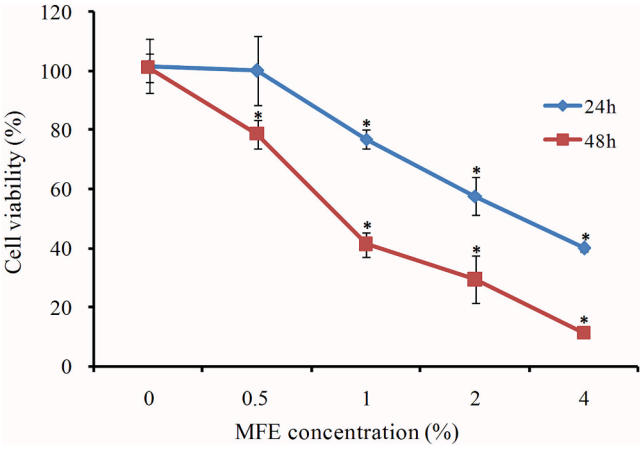

Fig. 1. The effect of different concentrations of MFE on the viability of BRL-3A cells measured by MTT assay. *P < 0. 05 vs control group (without MFE treatment).

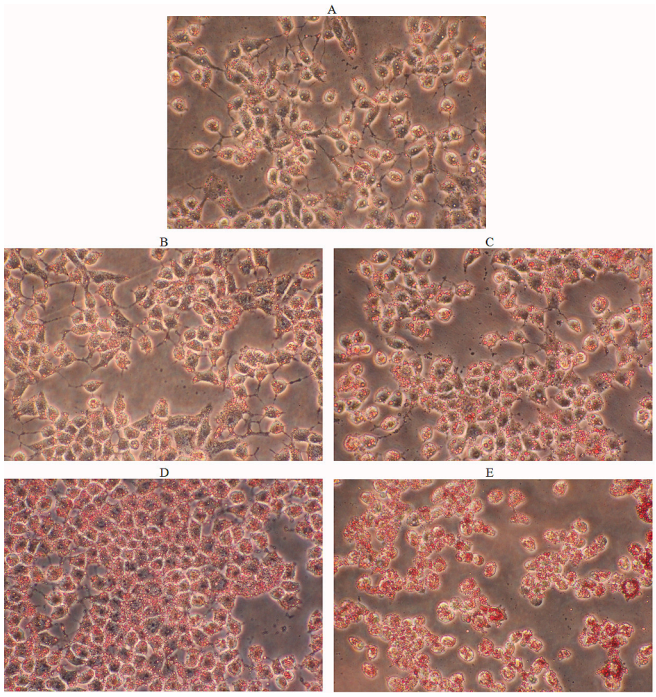

Fig. 2. Image of ORO staining of the cells treated with different concentrations of MFE for different time periods (100 × magnification) A: Control group; B,C: 0.5 % MFE treatment for 24 h and 48 h, respectively; D,E: 1 % MFE treatment for 24 h and 48 h, respectively.

After 0.5 % MFE treatment for 24 h, there was no significant change in the amount of lipid droplets compared to the normal group (Fig. 2B), while a moderate increase after 48 h (Fig. 2C). When treated with 1 % MFE for 24 h, numerous red lipid droplets appeared in the cells, obviously much more than that in 0.5 % MFE-treated cells (Fig. 2D); after 48 h, although there was a continuously significant increase in the accumulation of intracellular lipid droplets, a majority of cells were damaged severely with low cell viability (Fig. 2E). Based on above data, 1 % MFE treatment for 24 h was selected as the optimal concentration and treatment time for establishment of in-vitro fatty liver cell model.

Selection of effective siRNA fragment of PDHα1 gene

Three synthesized PDHα1 siRNA fragments were transfected into the established in-vitro fatty liver cells. After 24 h of transfection, the expression of green fluorescence protein was observed in all the groups under fluorescent microscope, indicating the effective transfection of all the siRNA fragments into the cells (Fig. 3).

Furthermore, the interference efficiency of three siRNA fragments was detected by using qPCR. As a result, PDHα1 mRNA levels in the cells transfected with three siRNAs decreased to 94 %, 15 % and 50 % of the control level, respectively. Statistical analysis showed that, except siRNA1, other two siRNA fragments, especially siRNA2 significantly reduced mRNA expression level of PDHα1 in the cells ($P < 0.05$). Therefore, siRNA2 was selected as the best interference fragment for subsequent experiments (Fig. 4).

Expression of PDHα1 protein in the cells after siRNA transfection

Expression and localization of PDHα1 protein in the siRNA transfected-cells was detected using immunofluorescence staining. The result showed that red fluorescence-labeled PDHα1 protein in all the groups was evenly distributed throughout the cell's cytoplasm under fluorescent microscopy; whereas the cells treated with siRNA for both 24 h and 48 h showed a decrease in the fluorescence intensity of PDHα1 as compared to the control and MFE-treated groups (Fig. 5, Fig.S1).

Furthermore, fluorescence density was analyzed for quantifying the level of PDHα1 protein in the cells interfered by siRNA. As shown in Table 3, the average fluorescence densities of control group and MFE-treated group were sequentially 0.123 and 0.128, with no significant difference between these two groups ($P > 0.05$). After interference for 24 h, the fluorescence density slightly decreased to 0.113 ($P > 0.05$), further significantly reduced to 0.087 ($P < 0.05$) after 48 h, indicating the lowest level of fluorescence intensity in the cells transfected with PDHα1 siRNA for 48 h.

Change in glucose metabolic activity in the cells after siRNA transfection

To evaluate the effect of interfering PDHα1 expression on glucose metabolic activity in the cells, this study examined the changes in lactate dehydrogenase (LDH) level in the cells and glucose content in culture medium. As shown in Table 4, LDH level in the cells from the control, MFE, and MFE + 24 h-interference groups were 1553.13, 1570.80 and 1580.73 mU, respectively, and the result of statistical analysis showed no significant difference between these three groups ($P > 0.05$). After 48 h of interference, LDH level dropped down almost to the normal again (1542.80 mU, $P > 0.05$). As for glucose consumption, glucose level showed a slight decrease ($P > 0.05$) in MFE group (245.43 ± 28.71 mg/dL) relative to that in control group (259.85 ± 45.49 mg/dL). After 24 h and 48 h of transfection, glucose content in the medium significantly increased ($P < 0.05$) from 245.43 ± 28.71 to 361.47 ± 12.78 mg/dL and 378.66 ± 4.43 mg/dL, respectively. This result indicated that siRNA transfection caused a time-dependent increase in glucose content in culture medium, implying a reduction in glucose consumption.

Change in lipid level after PDHα1 gene interference

Triglyceride (TG) content and lipase (LPS) activity in the cells were measured for evaluating the effect of PDHα1 gene silencing by RNA interference on lipid metabolism. The result showed that both TG content (3.426 ± 0.125 mmol/L) and LPS activity (27.563 ± 3.691 U/L) in MFE group were all higher than the control, and increased to about 1.8 and 1.6 folds of the control, respectively ($P < 0.05$). After interference for 24 h and 48 h, TG levels were remarkably reduced to 2.427 ± 0.231 mmol/L and 2.363 ± 0.351 mmol/L, respectively ($P < 0.05$); LPS activity slightly declined (24.130 ± 1.441 U/L, $P > 0.05$) at 24 h and then rise drastically (41.127 ± 1.973 U/L) at 48 h ($P < 0.05$, Table 5), demonstrating that the specific inhibition of PDHα1 expression by siRNA can enhance lipid catabolic process.

Changes in structure and function of mitochondria after PDHα1 gene interference

The mitochondrial ultrastructure after transfection of PDHα1 siRNA was observed under transmission electron microscopy (TEM). As shown in Fig. 6, the mitochondria in normal cells had the intergral structure with smooth outer membrane surface, and the tightly stacked and roughly parallel cristae with rich lamellae (Fig. 6A). The cells from MFE-treated group also had the mitochondrial structure similar to the control (Fig. 6B). After 24 h and 48 h of transfection, the cellular mitochondria had no significant ultrastructural change when compared with the control (Fig. 6C, 6D), indicating that interfering with PDHα1 expression has almost no influence on the mitochondrial structure.

Furthermore, cellular ATP level was assayed for examining the effect of interfering with PDHa1 gene on mitochondrial activity. The results, as shown in Table 6, indicated that ATP level (1.38 ± 0.05 μmol/gprot) had no significant change in MFE-treated group compared with the control (1.37 ± 0.03 μmol/gprot); after 24 h of transfection, ATP level obviously decreased to 0.89 ± 0.07 μmol/gprot ($P < 0.05$), while quickly and significantly increased to 1.10 ± 0.04 μmol/gprot after 48 h ($P < 0.05$).

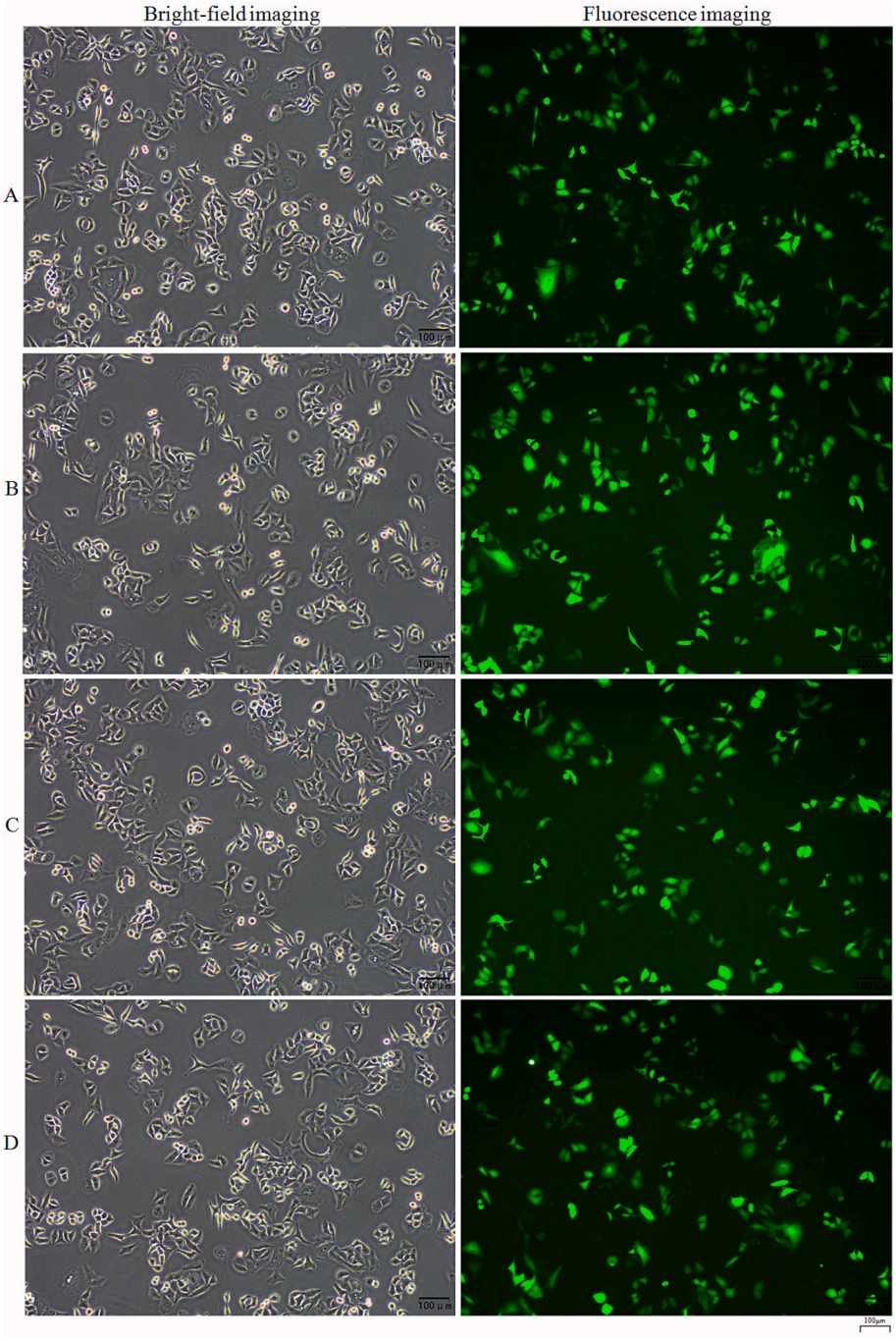

Fig. 3. Observation by fluorescence microscopy of GFP expression in the PDHα1 siRNA-transfected cells (Scale bar: 200 μm) A. FAM-negative control group; B-D. PDHα1 siRNA1, siRNA2 and siRNA3 transfection groups, respectively.

Discussion

As a rate-limiting enzyme, PDH catalyzes the irreversible oxidative decarboxylation of pyruvate to AcCoA, which enters into the TCA cycle to produce ATP and thus connects glycolysis with the TCA cycle (Saed et al., 2021). Studies have shown that PDH deficiency had very little impact on hepatocyte regeneration and liver cancer cell proliferation, implying that cutting the link between these two biochemical processes has a minimal impact cell growth (Choi et al., 2010; Karissa et al., 2022), from which we hypothesized that liver-specific knockout of PDH would lead to an increase in lipid expenditure instead of glycolysis for ATP generation and cell survival maintenance. Therefore, from the point of in vitro experimental study, in the present study, rat liver BRL-3A cells were selected for treatment with different MFE concentrations for different time, and the result showed that about 70 % of the cells cells remained at high viability even after 24 h of treatment with 1 % MFE, meanwhile, the cells showed a significant steatosis characterized by lipid droplet accumulation. After 48 h, lipid droplet number in the cells was significantly increased, but accompanied with low cell viability and severe cell necrosis. Consistently, through administrating human liver HL7702 cells with different concentrations of MFE ranging from 0.1 % to 4% for 24 h, Liu et al (2012) also considered 1 % MFE as the optimal induction concentration for establishing in vitro NAFLD cell model. Next, three siRNAs targeting PDHα1 gene were separately transfected into the constructed fatty liver cells, and qRT-PCR results observed the most significant decrease in PDHα1 mRNA level in the cells transfected

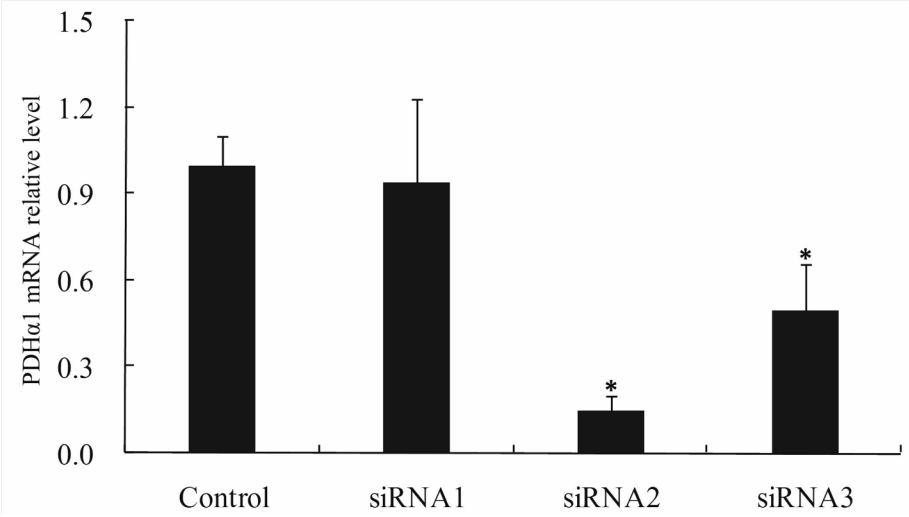

Fig. 4. The mRNA levels of PDHα1 in the cells after 24 h of siRNA transfection using qRT-PCR. *$P < 0.05$.

with siRNA2, indicating the most effective inhibitory effect of siRNA2 which thus was selected for the subsequent experiments.

Patel et al. (2012) found that PDH deficiency in infancy promotes the cytoplasmic reduction of pyruvate to lactate, resulting in lactate accumulation and varying degrees of metabolic acidosis. And this reaction is mainly catalyzed by lactate dehydrogenase (LDH) that acts as the terminal enzyme on glycolytic pathway. Our data showed that LDH level after 24 h of interference slightly increased compared with the control group and MFE-treated group; After 48 h of interference, LDH level again returned to the normal level, seemingly being not entirely consistent with Patel's findings, which could be explained that, interfering PDHα1 gene expression inhibits the conversion of pyruvate to AcCoA, and turns to promoting the conversion of pyruvate into lactate by increasing LDH activity; in turn, the accumulation of lactate exerts a feedback suppression on lactate production, with companion of inhibition on LDH activity. Coincidentally, the test result of glucose content in this experiment also showed that, with the prolongation of transfection time, the glucose levels in culture medium increased from 259.85 mg/dl in the control group to 361.47 mg/dl at 24 h and 378.66 mg/dl at 48 h, which implied that glucose utilization by the cells was reduced after interfering with the expression of PDHα1. Glucose is the main energy substrate and PDH complex is an important factor in regulating glucose homeostasis in the body. Early in 1980 s, Butterworth (1982) pointed out that PDH defect is generally accompanied with the decreased glucose utilization, which was consistent with our results. However, the findings of Gopal et al (2023) demonstrated that PDH deficiency dramatically augmented glycolytic pathway and switched pyruvate generation from glucose oxidation to lactate production by LDH, during which glucose uptake and utilization were promoted, but severe lactic acidosis was induced. The cause for the difference in the findings needs further scrutinizing, which might be related to the used detective methods, the timing of detection and so on.

Generally speaking, the amount of acetyl-CoA derived from glycolytic pathway determines the level of ATP synthesis in mitochondria (Zhou et al., 2018). Well, whether the reduction in glycolytic process impairs the production of ATP via oxidative phosphorylation? Based on our data, compared with MFE-treated group, cellular ATP level was dramatically increased after RNA interference against PDHα1, especially interference for 48 h ($P < 0.05$), implying that interfering PDHα1 gene can temporarily affect metabolic capacity of mitochondria to a certain extent, which was in agreement with Brown's findings (1994) that PDH activity decides the degree of energy substrate utilization, and that the activities of ATP synthesis-related enzymes directly affect the capacity of ATP generation. Furthermore, we observed the effect of interfering PDHα1 gene on mitochondrial structure, and there was no significant changes in mitochondrial morphology after RNA interference, which was consistent with Lu et al.'s result about the impact of obesity on mitochondrial structure and function (Lu et al., 2022). Taken together, no significant structural alteration in mitochondria occurred after inhibiting PDHα1 gene expression, and the temporary decrease and then rapid recovery in ATP content might be due to the gradually elevated metabolism of lipid.

As mentioned above, as for ATP level, the special change of descend firstly then recover may be theoretically related to the gradually accelerated lipid degradation. Coincidentally, we found a time-dependent and significant reduction in cellular TG level after RNA interference. As a key rate-limiting enzyme, LPS is a key driver in hydrolysis of triglycerides, and restraining the activity of this enzyme can directly affect the accumulation of lipid in the cells (Wang et al., 2023). Similarly, our study also detected the alteration of slight decrease (interference for 24 h) and then significant increase (interference for 48 h) of lipase activity, basically in accord with the changes in TG content, which may be explained that disconnecting glycolysis/TCA cycle by interfering PDHα1 gene would increase lipid catabolism and lower the TG level.

Conclusions

Based on above findings, inhibiting PDHα1 gene expression could attenuate glucose utilization by the cells, while facilitate lipid degradation which was mainly reflected by the elevated glucose level in the medium and the increased LPS activity, respectively; whereas the cellular energy produced by lipid degradation after interfering the expression of this gene might be not enough to compensate for the decrease of ATP level caused by the reduced glycolysis, which might be the reason for the short-time decrease of energy production.

Funding

This study was funded by Key scientific research projects of colleges and universities in Henan Province (No. 21A230001).

Institutional Review Board Statement

NA.

Informed Consent Statement

NA.

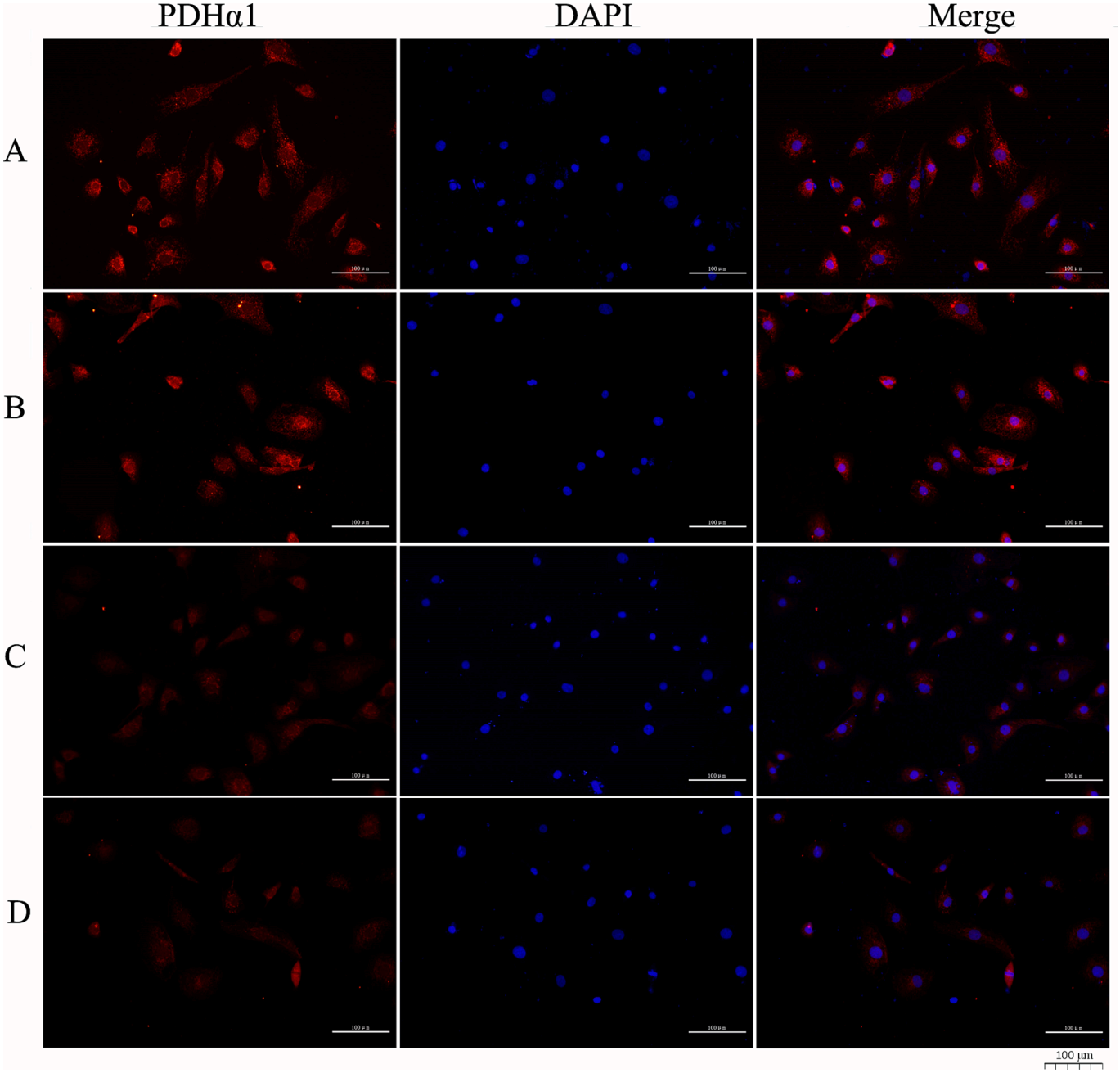

Fig. 5. Immunofluorescence detection of PDHα1 expression in the cells after siRNA transfection (Scale bar: 100 μm). A. Control group; B: MFE-treated group; C, D: MFE + RNAi groups (interference for 24 h and 48 h, respectively).

Table 3
Fluorescence density in the cells treated with PDHα1 siRNA.

Grouping	n	Optical density (OD)
Control	3	0.123 ± 0.009^{a}
MFE-treated	3	0.128 ± 0.009^{a}
MFE + RNAi (for 24 h)	3	0.113 ± 0.005^{a}
MFE + RNAi (for 48 h)	3	0.087 ± 0.010^{b}

Note: Different letters within the same column mean significant difference ($P < 0.05$); the same letters represent no significant difference ($P > 0.05$).

Table 4
Changes in levels of LDH and glucose in the cells after PHDα1siRNA transfection.

Grouping	LDH level (mU)	Glucose content (mg/dL)
Control	1553.13 ± 89.28	259.85 ± 45.49^{a}
MFE-treated	1570.80 ± 99.54	245.43 ± 28.71^{a}
MFE + RNAi (for 24 h)	1580.73 ± 70.94	361.47 ± 12.78^{b}
MFE + RNAi (for 48 h)	1542.80 ± 53.22	378.66 ± 4.43^{b}

Note: Different letters within the same column mean significant difference ($P < 0.05$); the same letters represent no significant difference ($P > 0.05$).

CRediT authorship contribution statement

Xiaoguang Chen: Investigation, Methodology, Validation, Writing – original draft. **Qiongxia Lv:** Investigation, Methodology, Validation, Writing – original draft. **Haonan Li:** Methodology, Validation, Visualization. **Zhe Wang:** Investigation, Methodology, Writing – original draft. **Yuxin Chang:** Investigation, Methodology, Writing – original draft.

Table 5
Changes in TG content and LPS activity in the cells after interfering PHDα1 gene.

Grouping	TG content (mmol/L)	LPS (U/L)
Control	1.922 ± 0.096[a]	17.063 ± 2.264[a]
MFE-treated	3.426 ± 0.125[b]	27.563 ± 3.691[b]
MFE + RNAi (for 24 h)	2.427 ± 0.231[c]	24.130 ± 1.441[b]
MFE + RNAi (for 48 h)	2.363 ± 0.351[c]	41.127 ± 1.973[c]

Note: Different letters within the same column mean significant difference ($P < 0.05$); the same letters represent no significant difference ($P > 0.05$).

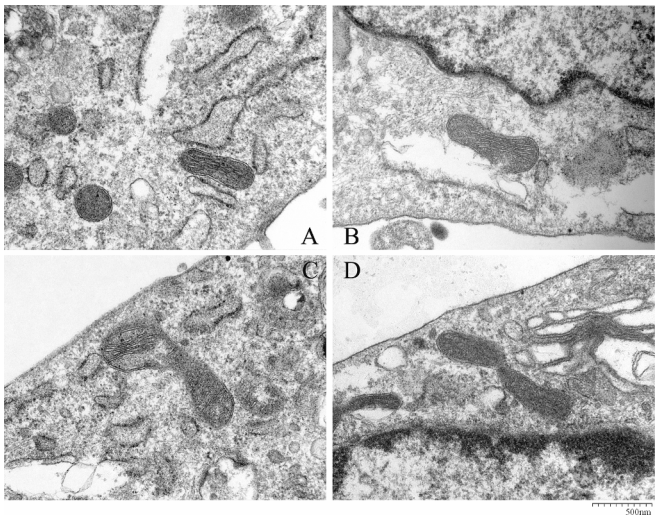

Fig. 6. TEM observation of mitochondrial ultrastructure (Scale bar: 500 nm). A: Control group; B: MFE-treated group; C, D: MFE + RNAi groups (interference for 24 h and 48 h, respectively).

Table 6
Change in ATP level after interference with PDHα1 siRNA.

Grouping	ATP level (μmol/10^6 cells)
Control	1.370 ± 0.030[a]
MFE-treated	1.377 ± 0.046[a]
MFE + RNAi (for 24 h)	0.886 ± 0.065[b]
MFE + RNAi (for 48 h)	1.097 ± 0.045[c]

Note: Different letters within the same column mean significant difference ($P < 0.05$); the same letters represent no significant difference ($P > 0.05$).

Declaration of competing interest

The authors declare that they have no known competing financial interests or personal relationships that could have appeared to influence the work reported in this paper.

Data availability

The authors do not have permission to share data.

Acknowledgements

We thank the funding support from the Key Scientific Research Project of Colleges and Universities in Henan Province (21A230001) and Student Research Training Program (SRTP) of Henan University of Science and Technology (2023491).

Appendix A. Supplementary data

Supplementary data to this article can be found online at https://doi.org/10.1016/j.crbiot.2023.100174.

References

Brown, G.K., Otero, L.J., LeGris, M., Brown, R.M., 1994. Pyruvate dehydrogenase deficiency. J. Med. Genet. 31 (11), 875–879.
Butterworth, R.F., 1982. Neurotransmitter functions in thiamine deficiency encephalopathy. Neurochem. Int. 4, 449–464.
Butterworth, R.F., 1989. Effects of thiamine deficiency on brain metabolism: implications for the pathogenesis of the Wernicke-Korsakoff syndrome. AlcoholAlcohol. 24 (4), 271–279.
Buttgereit, F., Brand, M.D., 1995. A hierarchy of ATP-consuming processes in mammalian cells. Biochem. J. 312 (Pt1), 163–167.
Choi, C.S., Ghoshal, P., Srinivasan, M., Kim, S., Cline, G., Patel, M.S., 2010. Liver-specific pyruvate dehydrogenase complex deficiency upregulates lipogenesis in adipose tissue and improves peripheral insulin sensitivity. Lipids 45 (11), 987–995.
Ciszak, E., Korotchkina, L.G., Hong, Y.S., Joachimiak, A., Patel, M.S., 2001. Crystallization and initial X-ray diffraction analysis of human pyruvate dehydrogenase. Acta Crystallogr. D Biol. Crystallogr. 57 (Pt3), 465–468.
Cooney, G.J., Denyer, G.S., Kerbey, A.L., Frankland, R.L., Blair, S.C., Williams, P.F., Caterson, I.D., 1990. Pyruvate dehydrogenase-complex activity in brown adipose tissue of gold thioglucose-obese mice. Biochem. J. 270 (1), 257–259.
Farrell, G.C., Chitturi, S., Lau, G.K., Sollano, J.D., Asia-Pacific Working Party on NAFLD, 2007. Guidelines for the assessment and management of non-alcoholic fatty liver disease in the Asia-Pacific region: executive summary. J. Gastroenterol. Hepatol. 22 (6), 775–777.
Fouret, G., Tolika, E., Lecomte, J., Bonafos, B., Aoun, M., Murphy, M.P., Ferreri, C., Chatgilialoglu, C., Dubreucq, E., Coudray, C., Feillet-Coudray, C., 2015. The mitochondrial-targeted antioxidant, MitoQ, increases liver mitochondrial cardiolipin content in obesogenic diet-fed rats. Biochim. Biophys. Acta 1847 (10), 1025–1035.
Gopal, K., Abdualkader, A.M., Li, X., Greenwell, A.A., Karwi, Q.G., Altamimi, T.R., Saed, C., Uddin, G.M., Darwesh, A.M., Jamieson, K.L., Kim, R., Eaton, F., Seubert, J. M., Lopaschuk, G.D., Ussher, J.R., Batran, A.I., R., 2023. Loss of muscle PDH induces lactic acidosis and adaptive anaplerotic compensation via pyruvate-alanine cycling and glutaminolysis. J. Biol. Chem. 299 (12), 105375.
Jackson, L.E., Kulkarni, S., Wang, H., et al., 2017. Genetic Dissociation of Glycolysis and the TCA Cycle Affects Neither Normal nor Neoplastic Proliferation. Cancer Res. 77 (21), 5795–5807.
Karissa, P., Simpson, T., Dawson, S.P., Low, T.Y., Tay, S.H., Nordin, F.D.A., Zain, S.M., Lee, P.Y., Pung, Y.F., 2022. Comparison between Dichloroacetate and Phenylbutyrate Treatment for Pyruvate Dehydrogenase Deficiency. Br. J. Biomed. Sci. 79, 10382.
Lane, A.N., Fan, T.W., 2015. Regulation of mammalian nucleotide metabolism and biosynthesis. Nucleic Acids Res. 43 (4), 2466–2485.
Liu, M., Kong, X.X., Yang, P., Chen, Y.B., Li, X.K., Wang, H.Y., 2012. Effect of fibroblast growth factor-21 on lipid metabolism of nonalcoholic fatty liver disease cell model induced in vitro. J. Jilin University (medicine Edition). 38 (3), 477–481.
Lu, Z.G., Wu, X.T., Huo, Q., Li, T., Lu, Y., Yin, H.Q., Wang, K., Du, Y., 2022. Maternal obesity causes neural tube dysplasia during mouse embryo development by influencing mitochondrial structure and function of neural progenitor cells. Chinese J. Pathophysiol. 38 (1), 87–95.
Matsumoto, M., Zhang, J., Zhang, X., Liu, J., Jiang, J.X., Yamaguchi, K., Taruno, A., Katsuyama, M., Iwata, K., Ibi, M., Cui, W., Matsuno, K., Marunaka, Y., Itoh, Y., Torok, N.J., Yabe-Nishimura, C., 2018. The NOX1 isoform of NADPH oxidase is involved in dysfunction of liver sinusoids in nonalcoholic fatty liver disease. Free Radic. Biol. Med. 115, 412–420.
Monteillet, L., Gjorgjieva, M., Silva, M., Verzieux, V., Imikirene, L., Duchampt, A., Guillou, H., Mithieux, G., Rajas, F., 2018. Intracellular lipids are an independent cause of liver injury and chronic kidney disease in non alcoholic fatty liver disease-like context. Mol. Metab. 16, 100–115.
Ni, H.M., Williams, J.A., Ding, W.X., 2015. Mitochondrial dynamics and mitochondrial quality control. Redox Biol. 4, 6–13.
Patel, K.P., O'Brien, T.W., Subramony, S.H., Shuster, J., Stacpoole, P.W., 2012. The spectrum of pyruvate dehydrogenase complex deficiency: clinical, biochemical and genetic features in 371 patients. Mol. Genet. Metab. 106 (3), 385–394.
Pelletier, J., Thomas, G., Volarević, S., 2018. Ribosome biogenesis in cancer: new players and therapeutic avenues. Nat. Rev. Cancer 18 (1), 51–63.
Ratziu, V., Harrison, S.A., Francque, S., et al., 2016. Elafibranor, an Agonist of the Peroxisome Proliferator-Activated Receptor-α and -δ, Induces Resolution of Nonalcoholic Steatohepatitis Without Fibrosis Worsening. Gastroenterology 150 (5), 1147–1159.
Saed, C.T., Tabatabaei Dakhili, S.A., Ussher, J.R., 2021. Pyruvate Dehydrogenase as a Therapeutic Target for Nonalcoholic Fatty Liver Disease. ACS Pharmacol. Transl. Sci. 4 (2), 582–588.
Sofou, K., Dahlin, M., Hallböök, T., Lindefeldt, M., Viggedal, G., Darin, N., 2017. Ketogenic diet in pyruvate dehydrogenase complex deficiency: short- and long-term outcomes. J. Inherit. Metab. Dis. 40 (2), 237–245.
Stacpoole, P.W., 2017. Therapeutic Targeting of the Pyruvate Dehydrogenase Complex/Pyruvate Dehydrogenase Kinase (PDC/PDK) Axis in Cancer. J. Natl. Cancer Inst. 109 (11).
Targher, G., Byrne, C.D., 2017. Non-alcoholic fatty liver disease: an emerging driving force in chronic kidney disease. Nat. Rev. Nephrol. 13 (5), 297–310.

Wang, J., Liang, G., Zhao, T.J., 2023. Adipose triglyceride lipase: the first transacylase for FAHFAs. Life Metab. 2 (1), loac016.
Wang, H., Lu, J., Kulkarni, S., Zhang, W., Gorka, J.E., Mandel, J.A., Goetzman, E.S., Prochownik, E.V., 2019. Metabolic and oncogenic adaptations to pyruvate dehydrogenase inactivation in fibroblasts. J. Biol. Chem. 294 (14), 5466–5486.
Zhou, Z., Austin, G.L., Young, L.E.A., Johnson, L.A., Sun, R., 2018. Mitochondrial Metabolism in Major Neurological Diseases. Cells 7 (12), 229.